Available online at www.sciencedirect.com
SCIENCE DIRECT
Catalysis Today 110 (2005) 264–271
CATALYSIS TODAY
www.elsevier.com/locate/cattod

Fe, Co and Cu-incorporated TUD-1: Synthesis, characterization and catalytic performance in N_2O decomposition and cyclohexane oxidation

M.S. Hamdy [a], G. Mul [a,*], W. Wei [a], R. Anand [b], U. Hanefeld [b], J.C. Jansen [c], J.A. Moulijn [a]

[a] *Reactor and Catalysis Engineering (R&CE), DelftChemTech, Technische Universiteit Delft, Julianalaan 136, 2628 BL, Delft, The Netherlands*
[b] *Gebouw voor Scheikunde, Technische Universiteit Delft, Julianalaan 136, 2628 BL, Delft, The Netherlands*
[c] *Ceramic Membrane Centre, "The Pore", DelftChemTech, Technische Universiteit Delft, Julianalaan 136, 2628 BL, Delft, The Netherlands*

Available online 26 October 2005

Abstract

Fe, Co and Cu-TUD-1 were prepared with different metal loadings (Si/M ratio = 100, 50, 20 and 10). As a function of increasing metal loading either isolated metal atoms, nano-particles of M-oxide and/or bulk M-oxide crystals in the silicate matrix were obtained, respectively. The materials were fully characterized by means of XRD, UV–vis, elemental analysis, N_2 sorption measurements and HR-TEM. The catalytic performance of the prepared materials was tested in gas phase N_2O decomposition and in liquid phase oxidation of cyclohexane. Results of N_2O decomposition showed that a low M-loading is beneficial for the catalysis and leads to a high TOF, Co-TUD-1 being the most active catalyst. This suggests that the nano-particles observed in many catalysts are not dominating the N_2O decomposition rate, and that active phase entities ranging from isolated to polynuclear sites are the most active. The performance of the TUD-1 catalysts is significantly lower than reported for the microporous Fe, Co and Cu analogues. In the oxidation of cyclohexane with TBHP, Cu-TUD-1 showed the highest activity but also significant leaching. Co-TUD-1 did not show any leaching and is thus the best applicable catalyst in cyclohexane oxidation.

Keywords: Fe; Co; Cu; TUD-1; Mesoporous; N_2O decomposition; Cyclohexane; Oxidation; TBHP

1. Introduction

The discovery of ordered mesoporous silica by Mobil scientists in 1992 [1,2] opened a new rich field in the world of catalysis. The importance of such materials derives from the fact that they posses a relatively large pore size compared to zeolites, which should allow the large molecules present in crude oil and in the production of fine chemicals to enter the pores and react. Consequently many mesoporous materials have been developed, such as the well known MCM-41, MCM-48, HMS-1 and SBA-15.

However, due to the absence of active sites in their matrices, siliceous mesoporous materials have to be functionalized. Different kinds of functionalization methods have been applied to mesoporous solids including attaching organometallic compounds and organic ligands [3,4]. Numerous metal oxides can be incorporated in mesoporous silicates, such as Ti, V, and Cr oxides [5,6], and many different approaches were described in the literature for inorganic functionalization of mesoporous materials [7].

TUD-1 (Technische Universiteit Delft) is one of the new mesoporous materials [8]. The synthesis of this mesoporous material is straightforward (one-pot procedure) and cost-effective because it is surfactant-free. TUD-1 has a 3D mesoporous structure which gives rise to a high accessibility for the substrates. Also TUD-1 can be functionalized with different

* Corresponding author. Tel.: +31 15 2784381; fax: +31 15 2785006.
E-mail address: g.mul@tnw.tudelft.nl (G. Mul).

0920-5861/$ – see front matter
doi:10.1016/j.cattod.2005.09.026

transition elements [9] such as Ti [10,11], Fe [12,13], and Co [14,15]. The catalytic activity of these materials in various reactions outperformed other mesoporous materials.

Nitrous oxide is a greenhouse gas and its emission forms the third largest contribution to global warming, after CO_2 and methane. N_2O emissions from the chemical industry are caused by a limited number of plants with large emissions, mainly nitric acid and adipic acid plants. The latter type of plants has been equipped with N_2O abatement technologies in recent years. The off gases of nitric acid plants contain significant amounts of water, oxygen and NO_x, and only ppm levels of nitrous oxide, rather than the percentage levels in the adipic acid plants. The presence of these components significantly deteriorates the performance of noble metal catalysts (Rh, Ru), which intrinsically have the highest N_2O decomposition activity [16–18]. Other, more cost-effective catalysts, such as Fe [19,20], Co [21,22] or Cu [23,24] based zeolites, have been evaluated extensively in the literature for their performance in N_2O decomposition, of which Fe is the most promising in nitric acid tail gas conditions, because of the promoting effect of NO on the N_2O decomposition rate. Mesoporous analogues of the zeolite catalysts (mainly ZSM-5) have not been studied extensively in relation to N_2O decomposition, besides Fe-MCM-41 [25], although also this study is more focussed on the characterization of the material, than on the catalytic performance [25].

Cyclohexane oxidation to cyclohexanone [K] and cyclohexanol [A] with a high selectivity is of great importance as these compounds are utilized in the manufacture of nylon-6 and nylon-6,6 [26,27]. Currently conversions have to be kept well below 10% in order to achieve reasonable selectivities and to avoid over-oxidation. For this selective oxidation of cyclohexane, cobalt is used as principle metal both in homogeneously and in heterogeneously catalyzed reactions. Industrially this reaction is carried out homogeneously at temperatures above 150 °C. Approximately 85% selectivity in mono-oxygenated products (a mixture of K, A, and cyclohexylhydroperoxide (CHHP)) is obtained. The development of new catalysts that achieve high conversions while maintaining high selectivity is thus a major challenge.

Here we introduce Cu-TUD-1 prepared analogously to Fe-TUD-1 and Co-TUD-1. The catalytic performance of the prepared materials was compared in gas phase N_2O decomposition and liquid phase cyclohexane oxidation with TBHP as an oxidant.

2. Experimental

2.1. Materials synthesis

Metal incorporated mesoporous materials, M-TUD-1 (M = Fe, Co and Cu) with a Si/M ratio of 100, 50, 20 and 10 were synthesized in a one-pot surfactant-free procedure based on a sol–gel technique using triethanolamine (TEA) as a bi-functional template and tetraethyl ammonium hydroxide (TEAOH) as a base [8]. The synthesis and characterization of Fe-TUD-1 is described elsewhere [12], as well as that of Co-TUD-1 [14,15]. In general, M-TUD-1 was synthesized according to the molar ratio 1 SiO_2:(0.01–0.1) M_xO_y:0.5 TEAOH:1 TEA:11H_2O. (The metal sources were: $Fe(NO_3)_3{\cdot}9H_2O$, $CoSO_4{\cdot}2H_2O$ and $Cu(NO_3)_2{\cdot}3H_2O$ all obtained from Aldrich and used without purification). In a typical synthesis example e.g. Cu-1 (cf. Table 1), a mixture of 24.7 g of TEA (97%, ACROS) and 6.5 g of deionized water was added drop-wise into a mixture of 33.2 g tetraethylorthosilicate (TEOS, 98% ACROS) and a copper salt solution (0.38 g of $Cu(NO_3)_2{\cdot}3H_2O$ in 3 ml deionized water) while stirring. Once the addition was complete, the solution was stirred for few minutes followed by addition of 33.2 g of TEAOH (35%, Aldrich). Then the mixture was aged at room temperature for 24 h, dried at 98 °C for 24 h, followed by a hydrothermal treatment at 180 °C for 8 h. Finally the solid products were calcined at 600 °C for 10 h with a ramp rate of 1 °C/min.

2.2. Characterization

X-ray powder diffraction (XRD) patterns were recorded using Cu Kα radiation on a Philips PW 1840 diffractometer equipped with a graphite monochromator. The samples were scanned over the range of 0.1–80° 2θ with steps of 0.02°. Nitrogen sorption isotherms were recorded on a Quantachrome Autosorb-6B at 77 K. Samples were previously evacuated at 623 K for 16 h and the BJH model was used to calculate mesoporosity from the adsorption branch of the N_2 adsorption–desorption isotherms. Diffuse reflectance (UV–vis) spectra were recorded using a CaryWin 300 spectrometer using $BaSO_4$ as reference. Samples were ground carefully, heated overnight at 180 °C, and then scanned from 190 to 900 nm. Elemental analyses were carried out by using instrumental neutron activation analysis (INAA) with a thermal power of 2 MW and maximum neutron reflux of $2 \times 10^{17}\ m^{-2}\ s^{-1}$. Transmission

Table 1
The elemental analysis and the N_2 adsorption measurements of Cu-TUD-1

Sample	Si/Cu ratio		S_{BET}[a] (m^2/g)	V_{meso}[b] (cm^3/g)	D_{meso}[c] (nm)	Colour
	Synthesis mixture	After calcination				
Cu-1	100	105	762	0.7	3.7	Grayish blue
Cu-2	50	49.1	718	0.7	4	Grayish blue
Cu-5	20	21.4	777	0.61	3.4	Gray
Cu-10	10	10.3	616	0.55	3.5	Gray

[a] Specific surface area.
[b] Mesopore volume.
[c] Mesopore diameter.

electron microscopy (HR-TEM) was carried out on a Philips CM30UT electron microscope with a field emission gun as the source of electrons operated at 300 kV. Samples were mounted on a copper-supported carbon polymer grid by placing a few droplets of a suspension of ground sample in ethanol on the grid, followed by drying under ambient conditions. EDX elemental analysis was performed using a LINK EDX system.

2.3. N_2O decomposition

The N_2O decomposition experiments were carried out in a six-flow reactor set-up. The set up was described in detail in [28]. The catalysts were ground and sieved to the size of 180–315 μm. Fifty milligrams of the catalyst was used without dilution with a space velocity (GHSV) of 36,000 h^{-1} at 3 bar. The feed condition used was 4.5 mbar N_2O with He as balance gas. Before reaction, the catalysts were pre-treated in He at 400 °C for 1 h and cooled to the initial reaction temperature. N_2O, N_2 and O_2 were analyzed with a GC (Chrompack CP9001) equipped with a thermal conductivity detector (TCD), using a Poraplot Q column and a Molsieve 5 Å column.

2.4. Cyclohexane oxidation

For the oxidation of cyclohexane with TBHP as oxidant, a stock solution of TBHP in cyclohexane was used, which had been prepared by extraction of commercial TBHP (Aldrich, 70% in water) into an equal volume of cyclohexane. Phase separation was promoted by saturation of the aqueous layer with solid NaCl. The organic layer was dried over $MgSO_4$, filtered and stored at 4 °C. In a typical experiment, M-TUD-1 containing 0.1 mmol active metal (pre-treated at 180 °C prior to the reaction) was added to 20 ml of a mixture of cyclohexane (65 mol.%), TBHP (35 mol.%) and 0.1 g chlorobenzene (used as internal standard). The round bottom glass flask with the reaction mixture containing the catalyst was then immersed in an oil bath at 70 °C. The gas phase above the reaction mixture was filled with nitrogen and a gas burette was attached. The course of the reaction was followed by analyzing the liquid samples on a GC. AAS analysis for leached metal ions in the filtrate obtained after cyclohexane oxidation experiments was performed on a Perkin-Elmer 4100ZL instrument. The reaction samples were analyzed using an Agilent 6890 gas chromatograph equipped with a split inlet (200 °C, split ratio 10.0) and using a Sil 5 CB capillary column (50 m × 0.53 mm I.D.; constant flow of carrier gas N_2 4.0 ml/min) coupled to an FID detector. The concentration of carboxylic acid side-products was determined from GC analysis by converting them into the respective methyl esters, as was described elsewhere [29].

3. Results and discussion

3.1. Cu-TUD-1, a new member in TUD-1 family

All Cu-TUD-1 samples with different Cu-loading (denoted as Cu-1, Cu-2, Cu-5, and Cu-10) were prepared at room temperature by using triethanolamine (TEA) as a bi-functional template which acts as a mesopore directing agent and as an anchoring agent (complexing ligand [30]) for copper active sites on the mesoporous wall. The copper contents in the synthesis gel and in the calcined product are summarized in Table 1. The Si/Cu ratio obtained after calcination in the final products is remarkably close to that present in the synthesis gel, which indicates that most of the copper cations are incorporated into the final solid product. Moreover, it demonstrates the high predictability of the synthesis method.

Fig. 1 shows the powder XRD patterns of various samples of Cu-TUD-1. All samples show a single intensive peak at 1–2.5° 2θ (Fig. 1A), indicating that Cu-TUD-1 is a meso-structured material. In addition, the high-angle powder XRD pattern (Fig. 1B) of Cu-1 did not show any detectable CuO phase or other crystalline phases. However, the patterns of Cu-5 and Cu-10 show additional peaks around 25 and 36° 2θ, which are consistent with the presence of a CuO crystalline phase.

Fig. 2 shows the N_2 sorption isotherms of the Cu-TUD-1 samples. All Cu-TUD-1 samples have type IV adsorption isotherms (Fig. 2A), indicating meso-structured character [31] with a narrow pore size distribution (Fig. 2B). In Table 1 the porosity measurements of the Cu-TUD-1 samples (calculated from the adsorption branch of the N_2 adsorption–desorption isotherms using the Barrett–Joyner–Halenda formula) are summarised: the surface area of the samples ranged from 616 to 777 m^2/g, the pore volume ranged from 0.5 to 0.7 cm^3/g and the mesopore diameter was estimated around 4 nm. While the pore

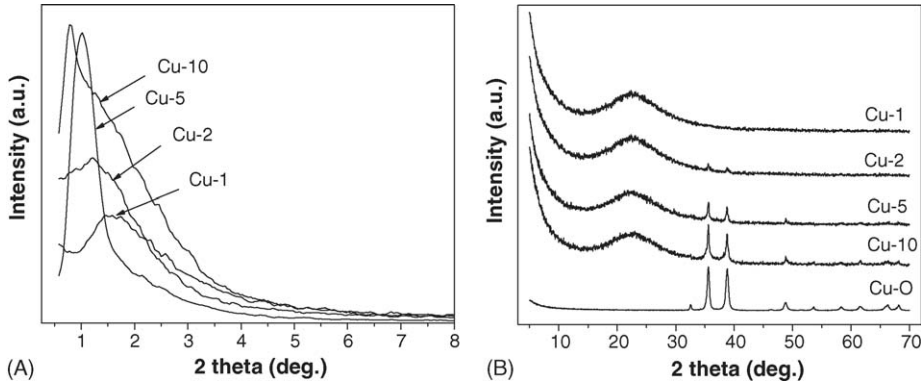

Fig. 1. X-ray diffractograms of Cu-TUD-1 samples. (A) low-angle patterns and (B) the high-angle patterns compared with CuO. Index as indicated in the figures.

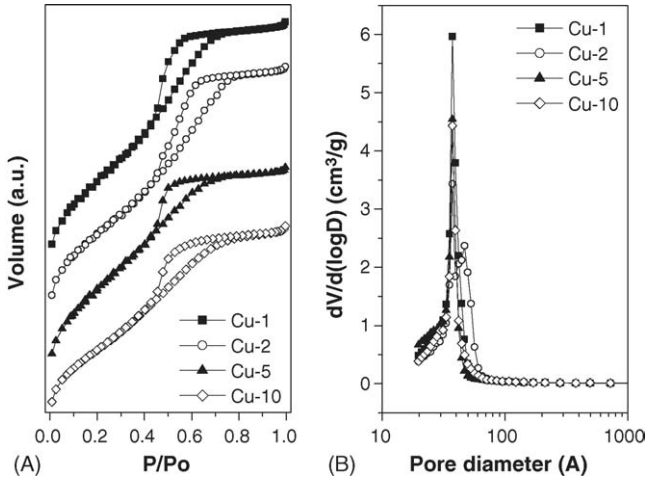

Fig. 2. (A) The N_2 adsorption isotherms and (B) the pore size distribution of different Cu-TUD-1 samples.

diameters are virtually independent of the Cu-loading, the pore volume decreased at higher Cu-loading, possibly due to CuO particles in the pores.

The UV–vis spectra of the calcined Cu-TUD-1 samples are shown in Fig. 3. The spectra are dominated by an intense band around 250 nm and two other broad bands around 460 and 750 nm, in addition to a shoulder around 304 nm associated with the Cu-10 sample. The broad band around 750 nm is assigned to the $^2E_g(D) \rightarrow {}^2T_{2g}$ transition of Cu^{2+} and this indicates the presence of a Cu^{2+} environment in a pseudo-octahedral coordination with 4–6 oxygen atoms in its first coordination sphere [32,33]. The strong band around 240 nm which shows a blue shift with increasing Cu-loading is attributed to the ligand to metal charge transfer (LMCT). The other broad band around 460 is due to the presence of polymeric $(Cu–O–Cu)_n$ species in 1D chains attached to the mesoporous walls [34]. More importantly, the shoulder around 304 nm in the Cu-10 sample is an indication of the presence of

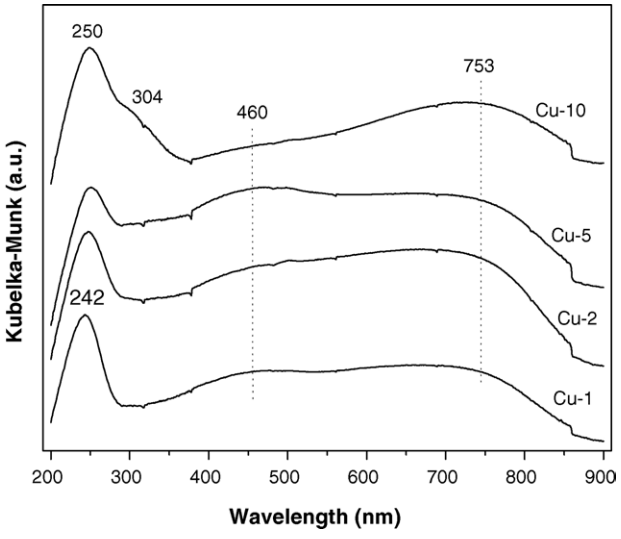

Fig. 3. The UV–vis spectra of Cu-TUD-1 samples. Legend as indicated in the figure.

CuO crystalline species. This is consistent with the XRD results.

Cu-TUD-1 samples were also investigated with high-resolution transmission electron microscopy (HR-TEM); many images were taken per sample. All the images of Cu-1 and Cu-2 (not presented here) showed only the sponge-like 3D structure characteristics of the TUD-1 mesoporous materials. This is a strong indication for the complete isolation of Cu atoms inside the framework. In the images of Cu-5 (Fig. 4) the diffraction fringes of CuO nano-crystals (in the range of 4 nm) were detected in addition to the sponge-like mesoporous matrix. Cu-10 images showed not only the mesoporous matrix and the nano-CuO particles, but also bulk CuO crystals, consistent with XRD and UV–vis data.

In conclusion, different active species (isolated sites, nano-particles and bulk crystals) were generated during the synthesis of Cu-TUD-1, as was also the case with Fe-TUD-1 [12] and Co-TUD-1 [15]. Table 2 summarizes the characteristics of the prepared M-TUD-1 samples (M = Fe, Co and Cu) as obtained from the different characterization techniques applied.

3.2. N_2O decomposition

The performance of the various Fe, Co and Cu-containing TUD-1 catalysts is shown in Figs. 5 and 6. Comparing the various TUD-1 based catalysts, for Fe-TUD-1 (Fig. 5A) and Cu-TUD-1 (Fig. 5B) the high M-loaded samples i.e. Fe-10 and Cu-10, respectively, show the highest activity on a per gram of catalyst basis. The behavior of the catalysts is somewhat different in the sense that for Fe the largest improvement is obtained by the increment of the loading of Fe from Fe-5 to Fe-10, while for copper the improvement is obtained by increasing the loading from Cu-1 to Cu-2. For Co-catalysts the enhancement of activity by increasing the metal loading is negligible (Fig. 5C). Comparing the samples with a high and low loading of the different elements incorporated into TUD-1 in Fig. 5D and E, respectively, indicates that Co is yielding the highest N_2O decomposition activity. At 600 °C, Co-10 decomposed 94% of the introduced N_2O, Fe-10 showed 65% conversion and Cu-10 showed only 50% conversion. This is specifically clear after correcting the activity for the M-loading, and plotting the turn over frequency (TOF) on a per metal atom basis (Fig. 6). For comparison, the performance of the bulk metal oxides is also included in Fig. 6. Generally, the catalysts with a low loading show the highest TOF. It is thus apparent that the active sites are created by introducing relatively small amounts of the active transition metals, while the addition of higher levels results in the formation of crystalline metal oxide particles that have a relatively small contribution to the overall N_2O decomposition. This is in agreement with results reported for Fe-ZSM-5 catalysts, in which crystals of Fe_2O_3 are generally reported to be of little importance in N_2O decomposition [16]. In this respect the increment in performance on a per gram of catalyst basis by increasing the Fe-loading from Fe-5 to Fe-10 in TUD-1 is unexpected and not very well understood (Fig. 5A). Two other aspects are of importance: (i) the role of the nano-particles in the catalyst

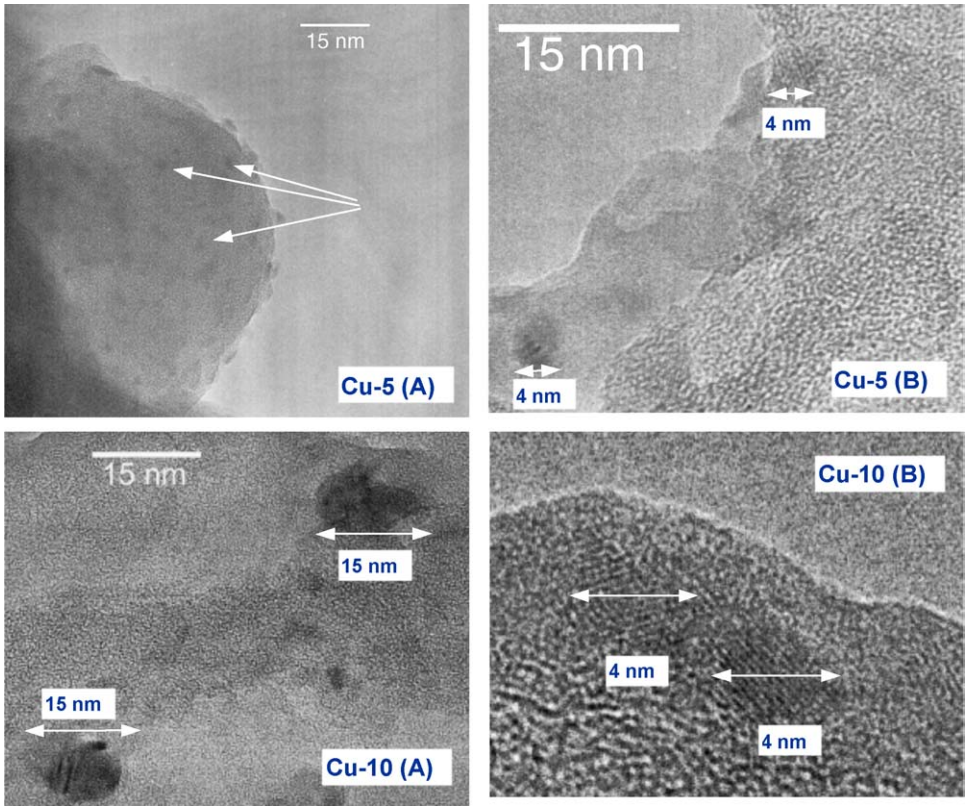

Fig. 4. HR-TEM images of Cu-5 and Cu-10 incorporated in TUD-1. Cu-5: (A) the arrows indicate CuO species well dispersed in the mesoporous matrix and (B) CuO species of ∼4 nm can be identified. Cu-10: (A) CuO particles of ∼15–20 nm and (B) the diffraction fringes of the ∼4 nm particles.

systems and (ii) the nature of the active site. By far the majority of the studies reported in the literature are dealing with Fe-based catalysts; hence the discussion will first focus on these. It was reported by Perez–Ramirez and others that after steaming of isomorphously substituted Fe-ZSM-5, nano-particles were obtained. The size range of these particles was somewhat smaller than observed for the TUD-1 samples, and the particles possess a more amorphous character [20]. In various studies on the so called ex-framework Fe-ZSM-5 [20] it was never excluded that these particles are of importance to the N_2O decomposition catalysis. Also the presence of Al in these particles appeared likely, and this led indirectly to the proposal that Al in vicinity of Fe is beneficial for the catalysis [35]. Because of the different nature of the nano-particles in steamed ZSM-5 catalysts and TUD-1 catalysts, conclusions related to the former system cannot be made. However, from the observed

Table 2
Iron, cobalt and copper as appeared in TUD-1

Sample	Si/M[a]	S_{BET}[b] (m^2/g)	Metal oxidation state	Metal co-ordination	Isolated sites	Metal oxide	
						Nano-particles[c]	Bulk crystals
Fe-1	113	568	Fe^{3+}	Tetrahedral	+	–	–
Fe-2	54	625	Fe^{3+}	Tetrahedral	+	–	–
Fe-5	21	803	Fe^{3+}	Tetrahedral	+	+(4–5 nm)	–
Fe-10	10.1	874	Fe^{3+}	Tetrahedral	+	+(2–3 nm)	–
Co-1	108	619	Co^{2+}	Tetrahedral	+	–	–
Co-2	47.8	605	Co^{2+}	Tetrahedral	+	–	–
Co-5	18.6	614	Co^{2+} + Co^{3+}	Tetrahedral	+	+(3–4 nm)	+
Co-10	9.95	684	Co^{2+} + Co^{3+}	Tetrahedral	+	–	+
Cu-1	105	762	Cu^{2+}	Pseudo- octahedral	+	–	–
Cu-2	49.1	718	Cu^{2+}	Pseudo- octahedral	+	–	–
Cu-5	21.4	777	Cu^{2+}	Pseudo- octahedral	+	+(3–4 nm)	–
Cu-10	10.3	616	Cu^{2+}	Pseudo- octahedral	+	+(3–4 nm)	+

[a] As obtained from elemental analysis for calcined samples.
[b] Specific surface area.
[c] The nano-particle size was determined by averaging at least 10 particles in HR-TEM images.

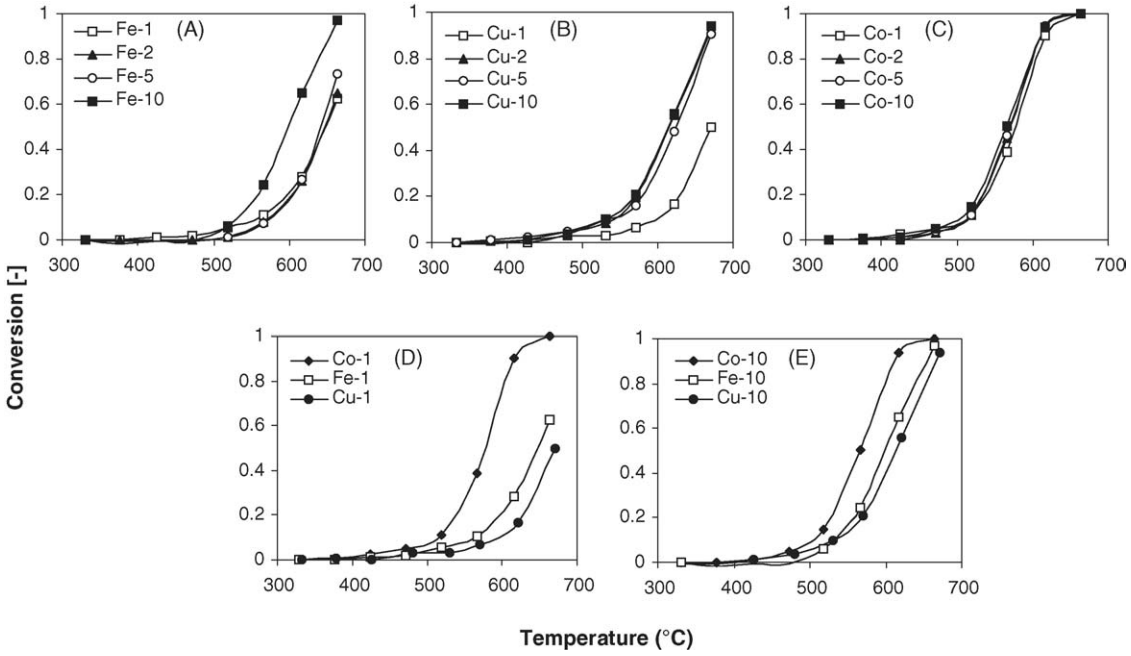

Fig. 5. N_2O conversion vs. temperature over Fe, Cu and Co-TUD-1. Legend as indicated in the figures. Conditions: 50 mg catalyst, GHSV 36,000 h^{-1}, 3 bar, 4.5 mbar N_2O in He.

relatively low activity in N_2O decomposition of the Fe-TUD-1 catalysts, these nano-particles embedded in the mesoporous TUD-1 structure appear to have a low contribution to the catalysis. Regarding the nature of the most active sites in the catalysts, Grubert [25] has recently reported a thorough analysis of Fe incorporated in Fe-MCM-41. Fe(II) species were identified in this system, and a peculiar reactivity towards N_2O was reported, yielding adsorbed NO at room temperature. It was also stated that in MCM-41, Fe was preferentially located at strained positions of the mesoporous structure. So far, the applied characterization techniques for Fe-TUD-1 provide too little detail to make firm conclusions of the nature and location of Fe in the framework of TUD-1, but in view of the relatively low activity it can be postulated that the number of redox active Fe-sites is significantly less in the TUD-1 matrix, than in the MCM-41 matrix. To improve the performance of Fe-TUD-1, currently two approaches are followed. First, in view of the previously mentioned beneficial effect of steaming on generating active sites in isomorphously substituted Silicalite and ZSM-5 based catalysts, the low loaded TUD-1 samples are exposed to such a treatment. Second, in view of the proposed enhancement of N_2O decomposition activity by combinations of Fe and Al in silicious matrices, combinations of Fe and Al incorporated in TUD-1 will be prepared and evaluated.

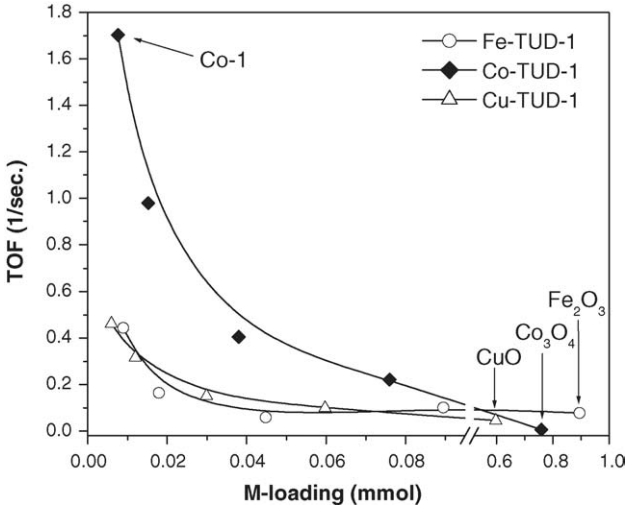

Fig. 6. The TOF of Fe, Co and Cu-TUD-1 in the N_2O decomposition reaction at 550 °C compared with Fe_2O_3, Co_3O_4 and CuO, respectively. The TOF was calculated on a per metal atom basis.

In view of the previous discussion, for Cu-TUD-1 it can also be postulated that Cu sites incorporated in the silicious matrix of TUD-1 induce the highest N_2O decomposition activity. Similar to Fe-based catalysts, most of the research in the use of Cu-based catalysts for N_2O decomposition has been directed at ZSM-5. In a recent study of Groothaert et al. [23] it was claimed that catalytic activity is predominantly induced by active species containing two copper ions. Measurement under transient reaction conditions indicated that $[Cu_2(\mu\text{-}O)_2]^{2+}$ is formed by O abstraction of N_2O. This conversion of N_2O to N_2 and O_2 is strongly retarded below 673 K. Above 673 K, the produced $[Cu_2(\mu\text{-}O)_2]^{2+}$ fulfills the role of O_2 release, guaranteeing the self-reduction of the catalytic site. The observed increment in catalytic performance in Fig. 5B, by increasing the loading from Cu-1 to Cu-2 might be related to this necessity of having neighbouring Cu-sites, although an increment of the 460 nm band in the respective UV–vis spectra is not obvious, and extended characterization, e.g. using the procedures of Groothaert et al. [23] are needed to support this hypothesis. CuO containing mesoporous silica structures have been reported previously by [36], who claim to have synthesized mesoporous silica spheres containing

nano-dispersed copper oxides. Temperature-programmed reduction and N_2O passivation procedures applied by the authors indicate that CuO clusters with increasing particle size could be formed in the mesoporous materials with increasing Cu contents, in agreement with our observations in TUD-1. This decreased the reducibility of the resulting CuO [36]. Since a redox cycle is beneficial for a high N_2O decomposition activity, a decreased reducibility of the CuO in TUD-1 with increasing loading might contribute to the decreasing TOF observed in the N_2O decomposition experiments (Fig. 6).

The catalytic performance of the Co-based TUD-1 materials, with an observed decreasing TOF as a function of increasing loading, can again be interpreted as that the isolated cobalt species in the matrix are inducing the activity in N_2O decomposition. Certainly Co-containing zeolites and ALPOs have been reported to be active and selective in redox reactions, which has been related to the ability to exchange between Co(II) and Co(III) oxidation states. The incorporation of Co species in a mesoporous matrix has not been abundantly documented, as was stated by [37], but it is likely that in TUD-1 also similar redox active sites as reported for the microporous materials are formed, explaining the high TOF at low Co-loading. Cobalt species in matrices such as MCM-41 have been evaluated by various characterization techniques, which indicate that Co atoms in MCM-41 are organized in well-dispersed, uniform CoO nano-domains of ca. 3 nm, partially embedded in the silica walls. Similar species were observed for Co incorporated in TUD-1 (referred to as nano-particles) [15]. Based on the activity data, it is not very likely that these nano-clusters dominate the N_2O decomposition activity.

Concluding, the obtained performance of the mesoporous M-TUD-1 was significantly lower than reported for the microporous ZSM-5 analogous [16], which is most likely related to a small contribution to N_2O decomposition of nano-particles and relatively large metal oxide particles on the one hand, and the relatively low redox cycle potential of the isolated or polynuclear sites of especially Fe and Cu in the TUD-1 matrix on the other.

3.3. Cyclohexane oxidation

In general, the oxidation of cyclohexane leads to cyclohexanol [A], cyclohexanone [K] and cyclohexylhydroperoxide [CHHP]. Also small amounts of cyclohexyl-*tert*-butylperether and cyclohexyl formate are observed. These products were grouped as mono-oxygenated products. In earlier experiments [15], it was found that isolated framework incorporated cobalt species in TUD-1 are active in the oxidation of cyclohexane. Here, the activity of isolated Co, Cu and Fe in the framework of TUD-1 is compared for the oxidation of cyclohexane with TBHP as oxidant. At 70 °C, both the conversion of cyclohexane (Fig. 7A) and TBHP (Fig. 7B) was catalyzed by all catalysts. The observed high rate of decomposition of TBHP over Cu-TUD-1 effects the conversion of cyclohexane more than observed for the other M-TUD-1 under study. However, selectivity for mono-oxygenated products drops sharply for both Cu- and Fe-TUD-1 suggesting that these catalysts are unable to prevent the formation of over-oxidation products (Fig. 7C). This trend is entirely different for Co-TUD-1: a very slow decrease in the selectivity for mono-oxygenated products is observed (Fig. 7C). The K/A ratio was either 1 or less than 1 (Fig. 7D) initially, suggesting that cyclohexanol is the major product. An increase of this ratio with time implies that cyclohexanol is also oxidized to cyclohexanone. A mixed

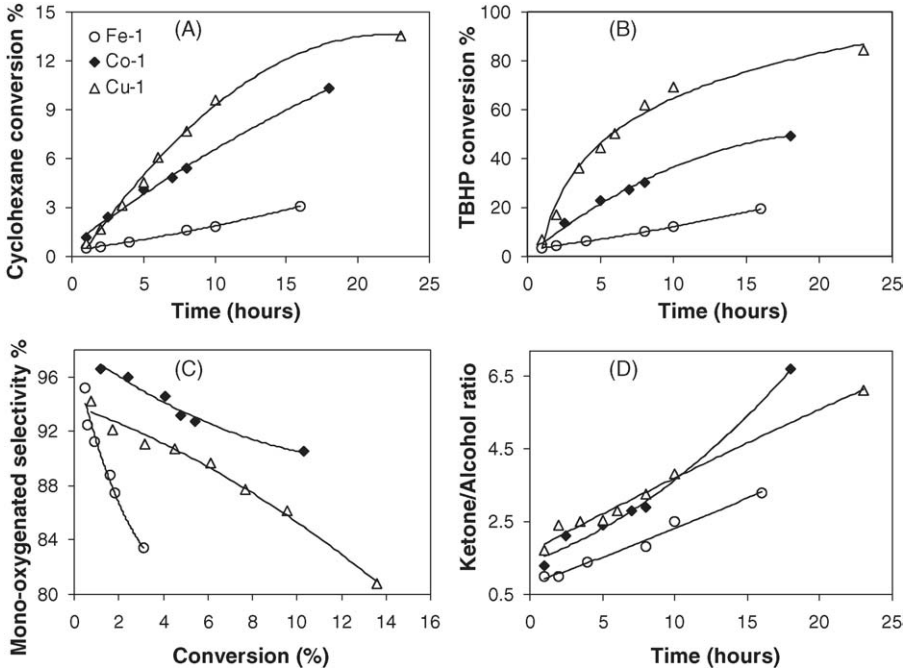

Fig. 7. The catalytic performance of Fe, Co and Cu-TUD-1 samples (Si/M ratio of 100) in cyclohexane oxidation with TBHP at 70 °C. Legend as indicated in the figures. (A) Cyclohexane conversion, (B) TBHP conversion, (C) selectivity for mono-oxygenated products, and (D) ketone/alcohol ratio.

Russell termination between cyclohexylhydroperoxy radicals and *tert*-butylhydroperoxy radicals could possibly also be responsible for the improvement of the K/A ratio. Due to the low yield and selectivity of mono-oxygenated products observed for Fe-TUD-1, the heterogeneity of the reaction was tested only for Co- and Cu-TUD-1. A straightforward procedure was adopted in which the reaction mixture was hot-filtered and the filtrate subjected to AAS analysis. This study revealed 0.5% leaching of Cu, while no Co was detected in the filtrate. Based on this and the foregoing discussion, it can be concluded that Co-TUD-1 is the catalyst of choice for oxidation of cyclohexane.

4. Conclusions

Cu-TUD-1 was synthesized successfully. The structure of the material as a function of transition metal loading is analogous to that previously reported for Fe-TUD-1 and Co-TUD-1 [12,15], which reflects the great flexibility of TUD-1 as a support for various transition elements. Characterization results prove that different active sites can be generated in M-TUD-1 (M = Fe, Co and Cu), ranging from isolated atoms incorporated within the TUD-1 silica matrix, to M-oxide nano-particles and/or bulk crystals of M-oxide. From the relation between the TOF and the applied transition metal loading, it can be concluded that the active phase entities ranging from isolated to polynuclear sites are the most active, and that the nano-particles have little contribution to the N_2O decomposition activity. Cu-TUD-1 was not as active as Co-TUD-1 in N_2O decomposition, however it showed the best conversion in cyclohexane oxidation. Unfortunately leaching of Cu was observed, while Co was not detected in the liquid phase. Hence, of the investigated TUD-1 materials, Co-TUD-1 with 1% Co-loading is the most promising catalyst for gas phase N_2O decomposition, as well as for liquid phase cyclohexane oxidation.

Acknowledgement

We thank Dr. P. Kooyman for HR-TEM study. M.S. Hamdy thanks the Ministry of High Education, Egyptian Government for the personal fellowship. U. Hanefeld and G. Mul gratefully acknowledge fellowships from the Royal Netherlands Academy of Arts and Sciences (KNAW).

References

[1] C.T. Kresge, M.E. Leonowicz, W.J. Roth, J.C. Vartuli, J.S. Beck, Nature 359 (1992) 71.
[2] J.S. Beck, J.C. Vartuli, W.J. Roth, M.E. Leonowicz, C.T. Kresge, K.D. Schmitt, C.T. Chu, D.H. Olsen, E.W. Sheppard, S.B. McCullen, J.B. Higgins, J.L. Schlenker, J. Am. Chem. Soc. 114 (1992) 834.
[3] G. Fryxel, J. Liu, Surf. Sci. Ser. 90 (2000) 665.
[4] K. Moller, T. Bein, Chem. Mater. 10 (1998) 295.
[5] T. Sun, J.Y. Ying, Nature 389 (1997) 704.
[6] P.T. Tanev, M. Chibwe, T.J. Pinnavaia, Nature 368 (1994) 321.
[7] L.M. Bronstein, Top. Curr. Chem. 226 (2003) 55.
[8] J.C. Jansen, Z. Shan, L. Marchese, W. Zhou, N. van der Puil, Th. Maschmeyer, Chem. Commun. (2001) 713.
[9] Z. Shan, M.S. Hamdy, J.C. Jansen, C. Yeh, P. Angevine, Th. Maschmeyer, (Delft University of Technology, ABB Lummus Global Inc.) (2003) U.S. Patent 2003188991;
Z. Shan, M.S. Hamdy, J.C. Jansen, C. Yeh, P. Angevine, Th. Maschmeyer, (Delft University of Technology, ABB Lummus Global Inc.) (2004) WO patent 2004052537.
[10] Z. Shan, J.C. Jansen, L. Marchese, Th. Maschmeyer, Micropor. Mesopor. Mater. 48 (2001) 181.
[11] Z. Shan, E. Gianotti, J.C. Jansen, J.A. Peters, L. Marchese, Th. Maschmeyer, Chem. Eur. J. 7 (2001) 1437.
[12] M.S. Hamdy, G. Mul, J.C. Jansen, A. Ebaid, Z. Shan, A.R. Overweg, Th. Maschmeyer, Catal. Today 100 (2005) 255.
[13] M.S. Hamdy, G. Mul, G. Hamminga, J.C. Jansen, J.A. Moulijn, Stud. Surf. Sci. Catal. 158B (2005) 1507.
[14] R. Anand, M.S. Hamdy, U. Hanefeld, Th. Maschmeyer, Catal. Lett. 95 (2004) 113.
[15] M.S. Hamdy, R. Anand, Th. Maschmeyer, U. Hanefeld, J.C. Jansen, Chem. Eur. J., in press.
[16] F. Kapteijn, J. Rodrigues-Mirasol, J.A. Moulijn, Appl. Catal. B 9 (1996) 25.
[17] S. Kawi, S.Y. Liu, S.C. Shan, Catal. Today 68 (2001) 237.
[18] K. Yuzaki, T. Yarimizu, K. Aoyagi, S. Ito, K. Kunimore, Catal. Today 45 (1998) 129.
[19] J. Perez-Ramirez, F. Kapteijn, G. Mul, J.A. Moulijn, Catal. Commun. 3 (2002) 19.
[20] J. Perez-Ramirez, F. Kapteijn, G. Mul, J.A. Moulijn, J. Catal. 208 (2002) 211.
[21] R.S. de Cruz, A.J.S. Mascarenhas, H.M.C. Andrade, Appl. Catal. 18 (1998) 223.
[22] S. Kannan, Appl. Clay Sci. 13 (1998) 347.
[23] M.H. Grootheart, K. Lievens, H. Leeman, B.M. Weckhuysen, R.A. Schoonheydt, J. Catal. 220 (2003) 500.
[24] Z. Schay, L. Guczi, G. Pal-Borbely, A.V. Ramaswamy, Catal. Today 84 (2003) 165.
[25] G. Grubert, M.J. Hudson, R.W. Joyner, M. Stockenhuber, J. Catal. 196 (2000) 126–133.
[26] W.B. Fisher, J.F. VanPeppen, in: M. Howe-Grant (Ed.), 4th ed., Kirk Othmer Encyclopedia of Chemical Technology, vol. 7, Wiley, New York, 1996, pp. 859–871.
[27] M.T. Musser in Ullmann's Encyclopedia of Industrial Organic Chemicals, vol. 3, VCH-Wiley, Weinheim, 1999, pp. 1807–1821.
[28] J. Perez-Ramirez, R.J. Berger, G. Mul, F. Kapteijn, J.A. Moulijn, Catal. Today 60 (2000) 93.
[29] M. Nowotny, L.N. Pedersen, U. Hanefeld, Th. Maschmeyer, Chem. Eur. J. 8 (2002) 3724.
[30] S. Teller, Y. Marcus, Y. Yan, Polyhedron 16 (1997) 1047.
[31] K. Sing, D. Everett, R. Haul, L. Moscou, R. Pierotti, J. Rouquerol, T. Siemieniewska, Pure Appl. Chem. 57 (1985) 603.
[32] S. Velu, L. Wang, M. Okazaki, K. Suzuki, S. Tomura, Micropor. Mesopor. Mater. 54 (2002) 113.
[33] V.F. Anufrienko, S.A. Yashnik, N.N. Bulgakov, T.V. Larina, N.T. Vasenin, Z.R. Ismagilov, Doklady Phys. Chem. 392 (2003) 67.
[34] Q. Xingyi, Z. Lili, X. Wenhua, J. Tianhao, L. Rongguang, Appl. Catal. A 276 (2004) 89.
[35] E. Hensen, Q. Zhu, P.-H. Liu, K.-J. Chao, R. Van Santen, J. Catal. 226 (2004) 466.
[36] L.Z. Wang, S. Velu, S. Tomura, F. Ohashi, K. Suzuki, M. Okazaki, T. Osaki, M. Maeda, J. Mater. Sci. 37 (2002) 801.
[37] J. El Haskouri, S. Cabrera, C.J. Gomez-Garcia, C. Guillem, J. Latorre, A. Beltran, D. Beltran, M.D. Marcos, P. Amoros, Chem. Mater. 16 (2004) 2805.